

Synthesis and Structure of Chemically Stable Metal–Organic Polyhedra

Zheng Lu, Carolyn B. Knobler, Hiroyasu Furukawa, Bo Wang, Guannan Liu, and Omar M. Yaghi*

Center for Reticular Chemistry, Department of Chemistry and Biochemistry, University of California–Los Angeles, 607 Charles E. Young Drive East, Los Angeles, California, 90095-1569

Received June 21, 2009; E-mail: yaghi@chem.ucla.edu

Metal–organic polyhedra (MOPs) have been extensively studied for their promising applications in the confinement of catalysts, otherwise unstable molecules and intermediates, drug delivery, and gas storage.^{1–4} Unlike extended porous frameworks, the solubility of MOPs offers many advantages for processing into thin films and as active additives in polymers.⁵ The chemistry of MOPs can be vastly expanded if they can be designed to display permanent porosity and chemical stability in acidic and basic media. We have shown that extended structures based on linking transition metals with imidazolate are porous and stable in refluxing organic solvents, boiling water, and hot concentrated sodium hydroxide solutions.⁶ Accordingly, we anticipated that their discrete analogues (MOPs based on transition metal imidazolates) would display similar porosity and stability with the added advantages provided by their solubility.

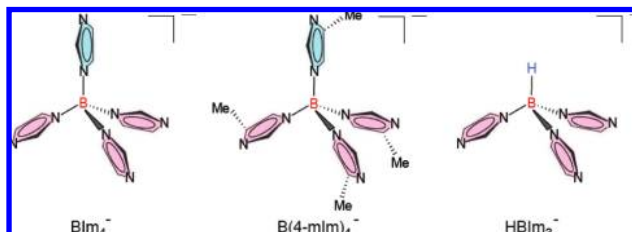
Here we report the synthesis and single crystal structures of two MOPs constructed by linking BIm_4^- and B(4-mIm)_4^- (Scheme 1) with palladium(II) into rhombic dodecahedra, termed MOP-100 and MOP-101, respectively. We describe their permanent porosity and their unusually high chemical stability in acidic and basic solutions.

A common method for the construction of a rhombic dodecahedral cage involves the linking of squares and triangles.^{7,8} We chose the Pd(II) ion as the square unit and the chemically stable linker BIm_4^- , which is known to be reactive at three imidazolates, to give the triangular unit (Scheme 1).⁹ We chose not to use HBIIm_3^- because of the lability of the B–H bond and the possible complications arising from side reactions that would destroy the required triangular symmetry.

The synthesis of MOP-100 and MOP-101 were carried out by combining equimolar amounts of $(\text{NH}_3)_4\text{Pd}(\text{NO}_3)_2$ (10% aqueous solution) and hydrogen tetrakis(1-imidazolyl)borate (HBIIm_4) or hydrogen tetrakis(4-methyl-1-imidazolyl)borate (HB(4-mIm)_4) in a concentrated ammonium hydroxide solution. The mixture was placed in a tightly capped vial and heated to 85 °C for 48 h to yield off-white crystalline $[\text{Pd}_6(\text{BIm}_4)_8](\text{NO}_3)_4 \cdot 10\text{H}_2\text{O}$ (MOP-100) or $[\text{Pd}_6\{\text{B(4-mIm)}_4\}_8](\text{NO}_3)_4 \cdot 14\text{H}_2\text{O}$ (MOP-101).¹⁰ Both MOP complexes were found to be sparingly soluble in polar solvents such as acetonitrile, methanol, and water.

The crystal structures of MOP-100 and MOP-101 (Figure 1) were determined by X-ray single-crystal diffraction studies.¹¹ Each MOP-100 cation cage is made up of six palladium ions and eight BIm_4^- representing squares and triangular vertices, respectively. The connectivity of the MOP-100 skeleton is similar to that of the reported spherical Pd_6L_8 cage with tritopic organic links and palladium(II) anions.⁸ The cage is electronically balanced by four nitrate anions, two inside the cage and two outside. It is worth noting that eight unbridged imidazolyl groups from eight BIm_4^- ligands, directed outside the cage, can serve as functional groups for further reactions. The X-ray crystallographic data for MOP-101 indicate the presence of several highly disordered imidazole groups and

Scheme 1. Triangular Linkers



distorted square planar geometry for the palladium ions. Nevertheless, MOP-101 unequivocally has a similar assembly to that of MOP-100.

Both ¹H NMR spectra of MOP-100 and MOP-101 in CD₃CN solution confirm the presence of two types of imidazolyl groups in both molecules with a peak integration ratio of 1:3 (unbridged/bridged), which are consistent with the crystal structures of the two MOPs.

It is difficult to model all the counteranions and the free guest molecules for MOP-101 using the X-ray single-crystal data due to the highly symmetrical and porous nature of the material (MOP-101 has about 41% solvent cavity).¹³ Hence, we examined the possibility of using the open space of MOP-101 for gas adsorption. N₂ adsorption measurements were performed on an evacuated sample of ethanol-exchanged MOP-101. The type I gas adsorption behavior is indicative of a microporous material (Figure 2A). From the adsorption branch of the isotherm, the Langmuir and BET surface areas were calculated to be 350 and 280 m² g⁻¹, respectively. The amount of N₂ uptake in the pores ($PIP_0 = 0.9$) corresponds to

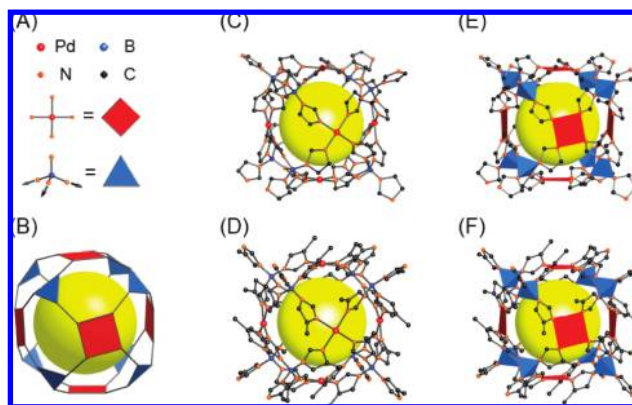


Figure 1. X-ray single-crystal structures of MOP-100/101 showing (A) PdN_4 and BN_4 units, (B) their underlying rhombic dodecahedron topology, ball and stick diagrams of (C) MOP-100 and (D) MOP-101, and polyhedral views of (E) MOP-100 and (F) MOP-101. The yellow spheres represent the largest sphere that would occupy the cavity without contacting the interior van der Waals surface (~ 7 Å).^{12,13} All hydrogen atoms, counteranions, and guest molecules have been omitted for clarity.

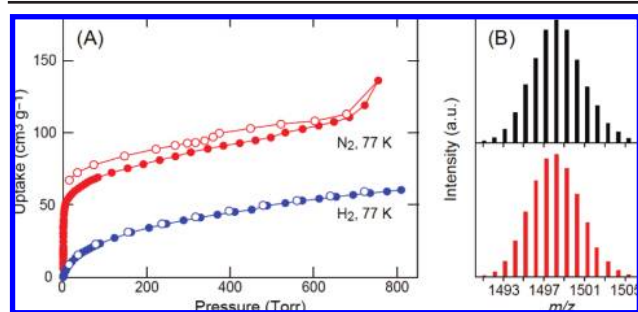


Figure 2. (A) N_2 (red) and H_2 (blue) isotherms at 77 K for MOP-101: filled and open circles represent the adsorption and desorption branches, respectively. Connected traces are guides for the eyes. (B) ESI-MS spectrum for $[\text{2NO}_3\subset\text{MOP-100}]^{2+}$: (black) experimental isotope patterns; (red) calculated isotope patterns.

17 N_2 molecules per rhombic dodecahedron. A small hysteresis in the N_2 isotherm is probably due to slow gas diffusion. The H_2 isotherm was also recorded for MOP-101 at 77 K, and 0.52 wt % of uptake at 1 bar was observed.

Since both MOPs are constructed from imidazolate–metal connections, we examined the chemical stability of these materials by suspending samples of the MOPs in organic solvents such as tetramethylethylenediamine, benzene, dichloromethane, methanol, *N,N*-dimethylformamide (DMF), dimethyl sulfoxide, and acetonitrile, at 85 °C or under reflux conditions for 24 h, after which electrospray ionization mass spectrometry (ESI-MS) data were collected for the solid samples. We note that the characteristic m/z 1497 and m/z 1724 in the ESI-MS spectra correspond to the intact cages of $[\text{2NO}_3\subset\text{MOP-100}]^{2+}$ (the symbol “ \subset ” indicates encapsulation) and $[\text{2NO}_3\subset\text{MOP-101}]^{2+}$, respectively (Figure 2B and Supporting Information). Thus, the observations for MOP-100 (m/z 1497) and MOP-101 (m/z 1724) for the solid samples in the ESI-MS studies confirmed the stability of the cage structures after treatment. A sample of MOP-100 was then immersed in 1 and 8 M KOH and 0.01, 0.1, and 1 M acetic acid aqueous solutions at 85 °C for 24 h, after which ESI-MS spectra and powder X-ray diffraction (PXRD) patterns were collected for the solid material recovered from the suspensions. All recovered samples retained the encapsulated cage structure ($[\text{2NO}_3\subset\text{MOP-100}]^{2+}$) as evidenced by the ESI-MS peak at m/z 1497. Furthermore, PXRD patterns for MOP-100 recovered from 1 M KOH and 0.01 M acetic acid solutions demonstrated that MOP-100 maintained its crystallinity under such conditions (Supporting Information). Indeed, the chemical stability of MOP-100 surpasses that of any palladium–pyridine based or polycarboxylate–metal based MOPs reported to date.^{1,2,4}

Although the rigid framework of MOP-100 protects the internal cavity under ESI-MS conditions, the accessibility of the internal cavity of MOP-100 has been confirmed by preliminary anion-exchange reactions. A MOP-100 sample was immersed into a DMF/ H_2O (2:1) solution containing an excess amount of NaCl, NaBr, or NaI at 85 or 120 °C for 24 h, after which ESI-MS spectra were collected for the reaction mixture. The result showed that no exchange reaction occurred for the iodide anion at either temperature. While the chloride and bromide anions did not exchange with nitrate anions in the cavity at 85 °C, we did observe such an exchange at 120 °C as evidenced by the presence of signals at m/z 1470 ($[\text{2Cl}\subset\text{MOP-100}]^{2+}$) and m/z 1515 ($[\text{2Br}\subset\text{MOP-100}]^{2+}$) (Supporting Information). Since the aperture of the MOP-100 cage in the crystalline state is less than 2 Å, we assume that the imidazolyl groups in the cage architecture are flexible enough to

open a pathway for the chloride and bromide anions at 120 °C and, consequently, to displace the nitrate anions. Since the larger-sized iodide anions are excluded from entering the cage cavity, it is clear that the MOP cage has anion size selectivity. Further anion selectivity tests of MOP materials are currently under investigation.

In summary, we have successfully synthesized and characterized two rhombic dodecahedral MOPs. Both exhibit exceptional chemical stability in common organic solvents as well as acidic and basic solutions. The permanent porosity of MOP-101 was confirmed by gas adsorption experiments. Anion exchange reactions demonstrated that the internal cavity of MOP-100 is accessible.

Acknowledgment. We thank Drs. C. J. Doonan and D. J. Tranchemontagne, and Messrs. D. Britt and Q. Li for helpful discussion. Funding was provided by DOD (HDTRA1-08-1-0023).

Supporting Information Available: Full synthetic procedures and characterization data. This material is available free of charge via the Internet at <http://pubs.acs.org>.

References

- (1) Olenyuk, B.; Leininger, S.; Stang, P. J. *Chem. Rev.* **2000**, *100*, 853–907. (a) Yoshizawa, M.; Sato, N.; Fujita, M. *Chem. Lett.* **2005**, *34*, 1392–1393. (c) Pluth, M. D.; Bergman, R. G.; Raymond, K. N. Selective Stoichiometric and Catalytic Reactivity in the Confinement of a Chiral Supramolecular Assembly. In *Supramolecular Catalysis*; Leeuwen, P. W. N. M., Ed.; Wiley-VCH: Weinheim, 2008; pp 165–191. (d) Leung, D. H.; Bergman, R. G.; Raymond, K. N. *J. Am. Chem. Soc.* **2007**, *129*, 2746–2747.
- (2) (a) Yoshizawa, M.; Kusukawa, T.; Fujita, M.; Yamaguchi, K. *J. Am. Chem. Soc.* **2000**, *122*, 6311–6312. (b) Yoshizawa, M.; Kusukawa, T.; Fujita, M.; Yamaguchi, K. *J. Am. Chem. Soc.* **2001**, *123*, 10454–10459. (c) Pluth, M. D.; Bergman, R. G.; Raymond, K. N. *J. Am. Chem. Soc.* **2008**, *130*, 6362–6366.
- (3) Perkin, K. K.; Turner, J. L.; Wooley, K. L.; Mann, S. *Nano Lett.* **2005**, *5*, 1457–1461.
- (4) (a) Ni, Z.; Yassar, A.; Antoun, T.; Yaghi, O. M. *J. Am. Chem. Soc.* **2005**, *127*, 12752–12753. (b) Sudik, A. C.; Millward, A. R.; Ockwig, N. W.; Côté, A. P.; Kim, J.; Yaghi, O. M. *J. Am. Chem. Soc.* **2005**, *127*, 7110–7118. (c) Furukawa, H.; Kim, J.; Ockwig, N. W.; O’Keeffe, M.; Yaghi, O. M. *J. Am. Chem. Soc.* **2008**, *130*, 11650–11661.
- (5) (a) Furukawa, H.; Kim, J.; Plass, K. E.; Yaghi, O. M. *J. Am. Chem. Soc.* **2006**, *128*, 8398–8399. (b) Abourahma, H.; Coleman, A. W.; Moulton, B.; Rather, B.; Shahgaldian, P.; Zaworotko, M. J. *Chem. Commun.* **2001**, 2380–2381. (c) Mohamed, K.; Abourahma, H.; Zaworotko, M. J.; Harmon, J. P. *Chem. Commun.* **2005**, 3277–3279.
- (6) (a) Park, K. S.; Ni, Z.; Côté, A. P.; Choi, J. Y.; Huang, R.; Uribe-Romo, F. J.; Chae, H. K.; O’Keeffe, M.; Yaghi, O. M. *Proc. Natl. Acad. Sci. U.S.A.* **2006**, *103*, 10186–10191. (b) Banerjee, R.; Phan, A.; Wang, B.; Knobler, C.; Furukawa, H.; O’Keeffe, M.; Yaghi, O. M. *Science* **2008**, *319*, 939–943. (c) Morris, W.; Doonan, C.; Furukawa, H.; Banerjee, R.; Yaghi, O. M. *J. Am. Chem. Soc.* **2008**, *130*, 12626–12627.
- (7) (a) Tranchemontagne, D. J.; Ni, Z.; O’Keeffe, M.; Yaghi, O. M. *Angew. Chem., Int. Ed.* **2008**, *47*, 5136–5147. (b) Berseth, P. A.; Sokol, J. J.; Shores, M. P.; Herinrich, J. L.; Long, J. R. *J. Am. Chem. Soc.* **2000**, *122*, 9655–9662. (c) Moon, D.; Kang, S.; Park, J.; Lee, Kyungjae; John, R. P.; Won, H.; Seong, G. H.; Kim, Y. S.; Kim, G. H.; Rhee, H.; Lah, M. S. *J. Am. Chem. Soc.* **2006**, *128*, 3530–3531.
- (8) Chand, D. K.; Biradha, K.; Fujita, M.; Sakamoto, S.; Yamaguchi, K. *Chem. Commun.* **2002**, 2486–2487.
- (9) Knop, O.; Bakshi, P. K. *Can. J. Chem.* **1995**, *73*, 151–160.
- (10) Microanalysis for $[\text{Pd}_6(\text{BIm})_4]_n(\text{NO}_3)_4 \cdot 10\text{H}_2\text{O}$, calcd: C, 34.95; H, 3.54; N, 28.87%. Found: C, 36.54; H, 3.33; N, 27.29%. For $[\text{Pd}_6(\text{B}(4\text{-mIm})_4)]_n(\text{NO}_3)_4 \cdot 14\text{H}_2\text{O}$, calcd: C, 43.04; H, 5.30; N, 25.09%. Found: C, 41.96; H, 4.84; N, 25.66%. See Supporting Information for details of synthesis.
- (11) Crystal data for MOP-100: space group $P\bar{1}$, $a = 19.4691(5)$ Å, $b = 19.7241(5)$ Å, $c = 23.4120(9)$ Å, $\alpha = 110.754(2)^\circ$, $\beta = 93.660(2)^\circ$, $\gamma = 116.55570(10)^\circ$, $Z = 2$, $\rho_{\text{calcd}} = 1.629$ g/cm³, 18 935 independent reflections observed; $R_1 = 0.0872$ (observed), $wR_2 = 0.2558$ (all data); MOP-101: space group $P4/mnc$, $a = b = 16.9134(3)$ Å, $c = 34.344(1)$ Å, $Z = 2$, $\rho_{\text{calcd}} = 1.258$ g/cm³, 1770 independent reflections observed; $R_1 = 0.0825$ (observed), $wR_2 = 0.1999$ (all data).
- (12) All measurements of distances were performed using *Cerius²* software; van der Waals radii were taken into consideration in all cases (Pd, 1.63; C, 1.70; H, 1.20; N, 1.55 Å). The yellow sphere represents the size of the largest molecule that may occupy the pore without contacting the van der Waals internal surface of the cage.
- (13) Solvent cavity was estimated by the CALC SOLV routine within the PLATON program with a probe radius of 1.20 Å; anions were excluded.

JA905101S